The HKU Scholars Hub The University of Hong Kong 香港大學學術庫

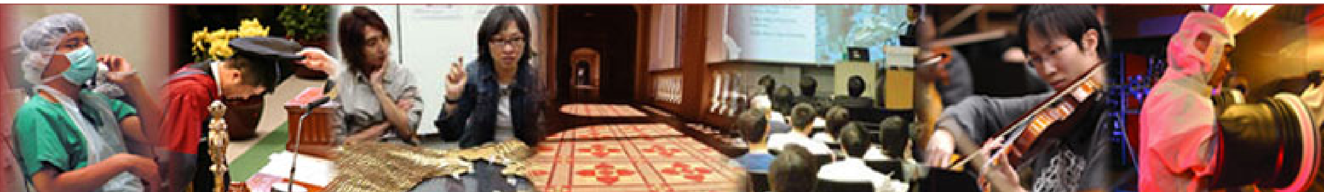

Title	Post-growth annealing induced change of conductivity in As-doped ZnO grown by radio frequency magnetron sputtering
Author(s)	To, CK; Yang, B; Su, SC; Ling, CC; Beling, CD; Fung, S
Citation	Journal Of Applied Physics, 2011, v. 110 n. 11
Issued Date	2011
URL	http://hdl.handle.net/10722/145575
Rights	Creative Commons: Attribution 3.0 Hong Kong License

Post-growth annealing induced change of conductivity in As-doped ZnO grown by radio frequency magnetron sputtering

C. K. To, B. Yang, S. C. Su, C. C. Ling,[a] C. D. Beling, and S. Fung
Department of Physics, The University of Hong Kong, Pokfulam Road, Hong Kong, People's Republic of China

(Received 6 July 2011; accepted 31 October 2011; published online 9 December 2011)

Arsenic-doped ZnO films were fabricated by radio frequency magnetron sputtering method at a relatively low substrate temperature of 200 °C. Post-growth annealing in air was carried out up to a temperature of 1000 °C. The samples were characterized by Hall measurement, positron annihilation spectroscopy (PAS), secondary ion mass spectroscopy (SIMS), and cathodoluminescence (CL). The as-grown sample was of *n*-type and it converted to *p*-type material after the 400 °C annealing. The resulting hole concentration was found to increase with annealing temperature and reached a maximum of $6 \times 10^{17}\,cm^{-3}$ at the annealing temperature of 600 °C. The origin of the *p*-type conductivity was consistent with the $As_{Zn}(V_{Zn})_2$ shallow acceptor model. Further increasing the annealing temperature would decrease the hole concentration of the samples finally converted the sample back to *n*-type. With evidence, it was suggested that the removal of the *p*-type conductivity was due to the dissociation of the $As_{Zn}(V_{Zn})_2$ acceptor and the creation of the deep level defect giving rise to the green luminescence. © *2011 American Institute of Physics*.
[doi:10.1063/1.3665713]

INTRODUCTION

ZnO is a wide bandgap material having physical properties suitable for fabricating UV-optoelectronic and spintronic devices.[1,2] It is generally known that defects play an important role in determining the optical and electrical properties of semiconductor materials. One of the important issues to address for successfully developing ZnO-based device technology is to overcome the asymmetric *p*-type doping difficulty of ZnO.[3,4] Many efforts have been devoted in this aspect, but reliable and reproducible p-type doping in ZnO has not yet been achieved. One of the important obstacles for achieving *p*-type doping in ZnO is the formation of compensating defects.[3,4] For the dopant arsenic, As_O is a deep acceptor and As_{Zn} is a donor, but the associated defect complex As_{Zn}-$2V_{Zn}$ is a shallow acceptor. All these aspects imply that a thorough understanding of defects, their evolution, and their inter-reaction is crucially important for achieving reliable *p*-type doping in ZnO. However, the understanding of defects in ZnO is far from complete.

Positron annihilation spectroscopy (PAS) is a probe selectively sensitive to neutral or negatively charged vacancy type defects, and it has been widely applied in studying vacancy in semiconductor materials.[5,6] Positrons injected into the solid would be rapidly thermalized and then undergo diffusion. The principle of PAS is that neutral or negatively charged vacancy would present as an attractive potential well to positron, and thus would trap the diffusing positron from its delocalized state. The electronic environment (namely, the electronic momentum distribution or the electronic density of the vacancy delocalized state) at which the positron annihilates is revealed by measuring the corresponding Doppler broadening of the annihilation radiation (DBAR) and the positron lifetime, respectively. PAS has been employed to study defects in various ZnO-related structures, such as ZnO bulk,[7–11] thin film,[12–14] nanorod structure,[15,16] metal-ZnO interface,[17,18] ion-implanted ZnO,[19,20] as well as defect related phenomenon, such as intrinsic defect associated ferromagnetism.[21]

We have recently carried out systematic study on fabricating arsenic doped *p*-type ZnO (Ref. 14) and ZnMgO (Ref. 22) films by radio frequency (RF) magnetron sputtering. It was found that the carrier conduction type and concentration were highly dependent on the substrate temperature during the growth process. *n*-type ZnO film was obtained at a low substrate temperature such as 200 °C. Reproducible *p*-type ZnO film having a hole concentration of $\sim 10^{18}\,cm^{-3}$ and a mobility of $\sim 6\,cm^2\,V^{-1}\,s^{-1}$ was only achieved with a critical substrate temperature (at 450 °C). The *n*-type to *p*-type conductivity conversion was attributed to the formation of the $As_{Zn}(V_{Zn})_2$ shallow acceptor complex and to the reduction of the hydrogen compensating donor.

In the present study, post-growth annealing study was performed on As-doped ZnO film grown at a low substrate temperature of 200 °C. *n*-type to *p*-type conversion was observed after the 400 °C annealing. The hole concentration increased after the 600 °C annealing. However, the hole concentration decreased and then returned to *n*-type if the annealing temperature further increased. PAS and cathodoluminescence (CL) were used to characterize the defects inside the materials in order to understand the mechanisms associated with the conductivity changes.

EXPERIMENTAL

Details of the RF magnetron sputtering growth are given in Refs. 14 and 22. With RF magnetron sputtering, the As-doped ZnO films used in the present study were grown on the SiO_2 substrates at a substrate temperature of 200 °C.

[a]Author to whom correspondence should be addressed. Electronic mail: ccling@hku.hk.

 © 2011 American Institute of Physics

Downloaded 15 Mar 2012 to 147.8.21.150. Redistribution subject to AIP license or copyright; see http://jap.aip.org/about/rights_and_permissions

The ceramic target contained Zn_3As_2 (1 mol %) and ZnO (99 mol %). The base pressure of the growth chamber was 10^{-3} Pa. The RF power was kept at 120 W. Secondary ion mass spectroscopy (SIMS) depth profiling measurements (Physical Electronics model 7200) showed that the fabricated film had a thickness of ~280 nm and the As atoms were uniformly distributed with a density of 10^{19}-10^{20} cm^{-3}. The Zn to O atomic ratio was 1.21. The X-ray diffraction XRD spectrum had a single peak at $2\theta = 34.47°$ (i.e., the ZnO (002) peak) and a fwhm = 0.19°, indicating the single phase wurtzite structure and the c-axis preferential orientation of the film. Post-growth annealing was carried out in a tube furnace in Ar atmosphere for a period of 30 min.

The Hall measurement was carried out with the Accent HL5500 system at room temperature using the van der Pauw configuration. The ohmic contacts for the Hall measurement were fabricated by depositing 50 nm Al films using the thermal evaporator. The room temperature CL measurement was conducted with the Oxford MonoCL system attached to the JEOL JSM-7001 F SEM.

The PAS measurement was conducted using the slow positron beam facility at the University of Hong Kong. The annihilation gamma ray energy spectra were collected using a high purity Ge detector and the corresponding nuclear electronics, which had an energy resolution of 1.3 keV at the 514 keV peak. The Doppler broadening of the annihilation gamma photons was monitored by way of the *S* and *W* parameters defined, respectively, as the ratios of the central window count and the summation of the two wings count to the total annihilation event count. The energy window for the *S*-parameter was 511 ± 0.76 keV and the two wing windows for the *W*-parameter were from 511 ± 3.4 keV to 511 ± 6.8 keV. *S*-parameter and *W*-parameter depth profiling of the sample was obtained by varying the positron beam energy *E* up to 20 keV. The *S-E* and *W-E* data were analyzed by the program VEPFIT,[23] which performed the fitting by assuming a Makhovian positron implantation profile and a layered sample structure, and considering the processes of positron diffusion, positron trapping into vacancies, and positron-electron annihilation.

RESULTS AND DISCUSSIONS

The carrier concentrations of the As-doped ZnO samples annealed at different temperatures are tabulated in Table I. The as-grown sample fabricated at the substrate temperature of 200 °C was *n*-type having $n = 5 \times 10^{16}$ cm^{-3}. After the post-growth annealing in Ar atmosphere at 400 °C, the sample converted to *p*-type having a hole concentration of $p = 2 \times 10^{17}$ cm^{-3}. The hole concentration then reached a maximum of $p = 6 \times 10^{17}$ cm^{-3} at the annealing temperature of 600 °C. Further increasing annealing temperature to 800 °C would reduce the hole concentration and the sample changed back to *n*-type after the 1000 °C annealing.

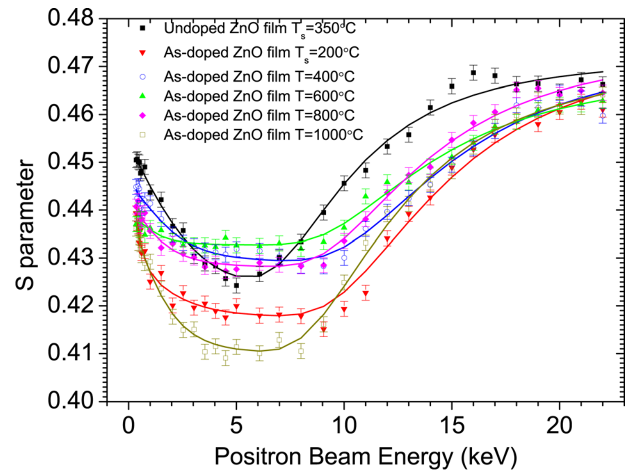

FIG. 1. (Color online) *S*-parameter as a function of the positron beam energy for the As-doped samples annealed at different temperatures. The curves are the fitted curves corresponding to the fitted parameters as shown in Table I.

The *S-E* data of the As-doped sample annealed at different temperatures were shown in Fig. 1. The *S-E* data (and also the *W-E* data) were fitted by the VEPFIT program with the assumption of the two-layer model. The fitted values of the *S*-parameter, *W*-parameter, and effective positron diffusion length L_+ are tabulated in Table I. The fitted curves are shown in Fig. 1, which indicate good fitting to the experimental data. The fitted *S* and *W*-parameters for the samples annealed at different temperatures were also shown in the *S-W* plot in Fig. 2 with the fitted L_+ labeled.

From Fig. 2, the *S* parameter and the *W* parameter of the as-grown sample were 0.417 and 0.0938, respectively. With the annealing temperature $T_{anneal} \leq 600$ °C, the *S*-parameter and *W*-parameter, respectively, increased and decreased with the increasing annealing temperature. The minimum value of $S = 0.433$ and the maximum value of $W = 0.0870$ were observed after the sample was annealed at 600 °C. The positron diffusion length L_+ simultaneously decreased from the

TABLE I. Summarizing the conduction type, the carrier concentration, and the fitted results of the *S-E* data (i.e., the *S*-parameter, the *W*-parameter, and the effective positron diffusion length L_+) for the samples annealed at different temperatures.

Annealing temperature	As-grown (substrate temperature = 200 °C)	400 °C	500 °C	600 °C	800 °C	1000 °C
Conduction type and carrier concentration	$n = 5 \times 10^{16}$ cm^{-3}	$p = 2 \times 10^{17}$ cm^{-3}	$p = 3 \times 10^{17}$ cm^{-3}	$p = 6 \times 10^{17}$ cm^{-3}	$p = 4 \times 10^{16}$ cm^{-3}	$n = 1 \times 10^{16}$ cm^{-3}
Fitted results of PAS data	$S = 0.4173$ $W = 0.09384$ $L_+ = 27$ nm	$S = 0.4290$ $W = 0.08830$ $L_+ = 21$ nm		$S = 0.4326$ $W = 0.08702$ $L_+ = 8$ nm	$S = 0.4280$ $W = 0.09083$ $L_+ = 16$ nm	$S = 0.4097$ $W = 0.1019$ $L_+ = 17$ nm

Downloaded 15 Mar 2012 to 147.8.21.150. Redistribution subject to AIP license or copyright; see http://jap.aip.org/about/rights_and_permissions

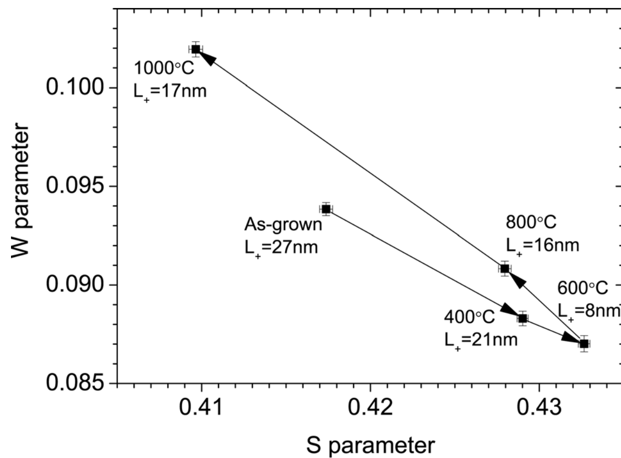

FIG. 2. *S*-parameter as a function of the *W*-parameter for samples annealed at different temperatures. The effective diffusion lengths L_+'*s* for each of the samples were included.

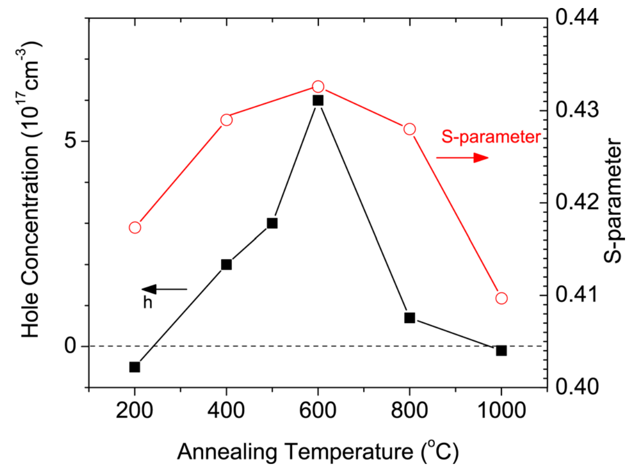

FIG. 3. (Color online) Hole concentration and S-parameter of the film as a function of the annealing temperature.

as-grown sample of 27 nm to the minimum of 8 nm of the 600 °C annealed sample. It is generally accepted that Zn-vacancy related defect and the relevant vacancy cluster are effective positron traps in ZnO at room temperature. Positron annihilating from these localized states would yield a higher *S*-parameter (and lower *W*-parameter and L_+) as compared to the delocalized state. On the other hand, oxygen vacancy has a much smaller positron binding energy of ~0.01 eV (~0.50 eV for V_{Zn}) and thus thermal detrapping of positron from V_O is significant at the room temperature. Therefore, the observed increase in *S*-parameter, and the decreases in *W* parameter and positron diffusion length with respect to T_{anneal} in the range of $T_{anneal} \leq 600\,°C$ simply implied the increase of V_{Zn}-related defect concentration and/or the increase of the vacancy open volume. In the range of $T_{anneal} > 600\,°C$, *W* decreased, *S* and L_+ increased with increasing T_{anneal}. This could be explained by the decrease of the open volume of the V_{Zn}-related defect and/or the thermal removal of the V_{Zn}-related defect. The *S*-parameter and the hole concentration of the samples were also plotted together against the annealing temperature in Fig. 3. The as-grown sample was *n*-type conducting. The *S*-parameter and the hole concentration increased with T_{anneal} for $T_{Anneal} \leq 600\,°C$, but they decreased while the annealing temperature further increased. The correlation between the *S*-parameter and the hole concentration was clearly demonstrated.

In the previous study of fabricating As-doped ZnO using the similar technique which involved the investigation of the effect of the substrate temperature, we have reported that the film grown at low substrate temperature (200 °C) was *n*-type. The conduction type of the sample changed to *p*-type ($p \sim 10^{17}\,cm^{-3}$) as the substrate temperature increased to 350 °C, then rose to the maximum of $\sim 10^{18}\,cm^{-3}$ while the substrate temperature increased to 400 °C. Further increasing the substrate temperature would decrease the hole concentration. Free electron to acceptor (FA) emission (3.282 eV) was identified in the low temperature (10 K) photoluminescence (PL) spectra of the As-doped *p*-type samples and the acceptor binding energy was thus found to be $E_A = 155$ meV. This value agreed well with the theoretical value of $\varepsilon(0/-) = 0.15$ eV of the $As_{Zn}(V_{Zn})_2$ acceptor,[24] and thus the shallow acceptor was attributed to this defect. XPS was also employed to study the occupying site of the As-atom in the ZnO lattice by monitoring the As (3 d) binding energy. For the As-doped ZnO samples grown by the RF magnetron sputtering, a single dominant peak of ~45 eV was found. This peak corresponded to the As-O bond rather than the As-Zn bond (~41 eV), thus indicating that the majority of the As-atom occupied the Zn-site in the ZnO lattice. This implied that the introduced As dopant formed a defect containing the As_{Zn} microstructure, which also agreed with the proposed $As_{Zn}(V_{Zn})_2$ shallow acceptor model. Moreover, the S-parameter of the As-doped ZnO film also rose with the hole concentration as the substrate temperature was increased. This was thought to be related to the open volume increase of the Zn-vacancy. According to the first principle calculation of the $As_{Zn}(V_{Zn})_2$ structure, the O-atom sitting adjacent to the As atom and the Zn-vacancy would be relaxed toward the As-atom. This atomic relaxation would lead to the increase of the Zn-vacancy open volume.

In Fig. 3, the *n*-type film was converted to *p*-type after the 400 °C annealing and the hole concentration increased further while the annealing temperature reached 600 °C. These observations were associated with the formation of the $As_{Zn}(V_{Zn})_2$ shallow acceptor. The corresponding increase of *S*-parameter was due to the increase of V_{Zn} open volume originated from the atom relaxation of the $As_{Zn}(V_{Zn})_2$ defect.

However, as shown in Fig. 3, further increasing the annealing temperature would decrease the hole concentration and the *S* parameter. The decrease of the hole concentration could be due to the formation of compensating defects and/or the thermal dissociation of the $As_{Zn}(V_{Zn})_2$ shallow acceptor at high annealing temperature. The corresponding decrease of the *S*-parameter supported the idea of the dissociation of $As_{Zn}(V_{Zn})_2$. It is because the resultant isolated V_{Zn} has a smaller volume than the V_{Zn} attached to the $As_{Zn}(V_{Zn})_2$ and thus would lead to the decrease of the *S*-parameter. We have also carried out XPS measurement on the 1000 °C annealed As-doped sample and the As (3 d) XPS spectrum still contained the 45 eV single peak, thus implying that the

Downloaded 15 Mar 2012 to 147.8.21.150. Redistribution subject to AIP license or copyright; see http://jap.aip.org/about/rights_and_permissions

majority of the As-atom remained as the As_{Zn} structure. It is thus plausible to suggest that the $As_{Zn}(V_{Zn})_2$ acceptor complex decomposes into isolated Zn-vacancy and As_{Zn} substitute defect.

It is also worth estimating the annealing temperature from the theoretical binding energy of $As_{Zn}(V_{Zn})_2$ and comparing it with the experimental findings. The frequency for a nearby atom jumping to a vacancy is given by $\Gamma = \Gamma_0 \exp(-E_b/kT)$, where E_b is the corresponding energy barrier, and Γ_0 is the vibration frequency from the initial configuration to the configuration corresponding to the saddle point. Taking $\Gamma = 1\,s^{-1}$, $\Gamma_0 = 10^{13}\,s^{-1}$ (which is a typical phonon frequency) (Ref. 25, and references therein), and $E_b = 2.84$ eV for the $As_{Zn}(V_{Zn})$,[24] the annealing temperature was found to be ~800 °C, which agreed with the drop-off temperature for the hole concentration and *S*-parameter (Fig. 3).

The SIMS depth profile of the Si, Zn, and O for the as-grown and the 800 °C annealed samples are shown in Figs. 4(a) and 4(b), respectively. As shown in Fig. 4(a), Si-Zn inter-mixing was found at the as-grown ZnO/SiO_2 boundary with a width of ~30 nm. After the 800 °C annealing, Zn diffused into the SiO_2 extending to a depth of about 60 nm the Si atom diffused into the whole ZnO film. This would inevitably introduce defects in the interface as well as in the whole ZnO film.

CL measurements were carried out on the samples annealed at different temperatures using two different electron beam energies, namely $E_b = 5$ keV and 10 keV. According to the empirical equation of Everhart and Hoff,[26] the electron penetration range R_e (in μm) is given by $R_e = (0.0398/\rho)E_b^{1.75}$, where ρ is in g cm^{-3} and E_b is in keV. The electron energy of 5 keV and 10 keV adopted in the present CL study of ZnO thus corresponded to the penetration depths of 120 nm and 390 nm, respectively. As the ZnO film thickness was ~300 nm, the CL spectrum obtained from $E_b = 5$ keV thus involved the majority of the luminescence originated from the front half of the sample, while that from $E_b = 10$ keV involved luminescence originated from the whole ZnO film, and the ZnO/SiO_2 interface.

Figures 5(a) and 5(b) are the CL spectra of the As-doped ZnO samples obtained from the electron beam energy $E_b = 5$ keV and 10 keV, respectively. For the $E_b = 5$ keV spectrum, three peaks at 1.6 eV, 2.5 eV, and 3.2 eV were identified. These three peaks were also found in the $E_b = 10$ keV spectrum of the samples. In addition, two other peaks (2.8 eV and 3.0 eV) were only identified in the $E_b = 10$ keV spectra.

The near-band-edge emission 3.2 eV was observed in all of CL spectra. Annealing had the effect of increasing its intensity, which could be due to the removal of the non-

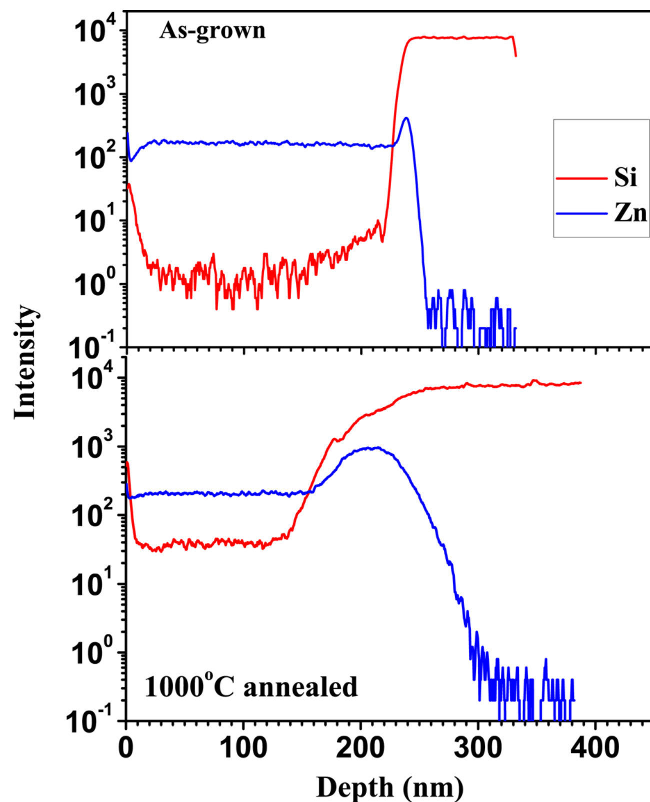

FIG. 4. (Color online) SIMS depths of Si and Zn for the as-grown and the 1000 °C annealed As-doped ZnO samples.

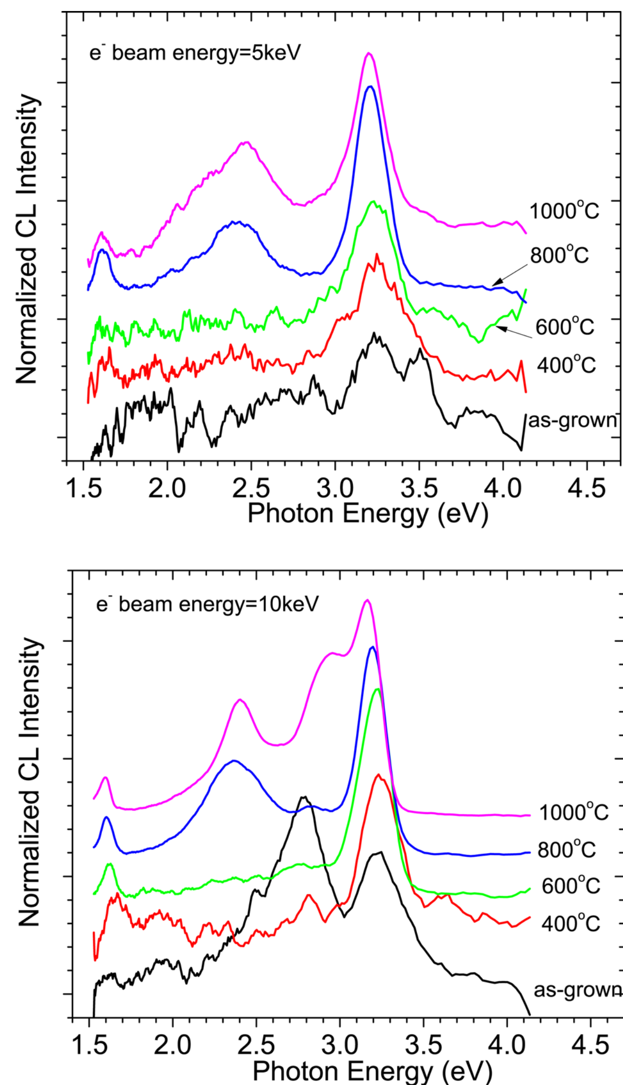

FIG. 5. (Color online) CL spectra of the samples annealed at different temperatures with the electron beam energy equal to (a) 5 keV and (b) 10 keV.

Downloaded 15 Mar 2012 to 147.8.21.150. Redistribution subject to AIP license or copyright; see http://jap.aip.org/about/rights_and_permissions

radiative defects and the improvement of the crystalline quality.

As shown in the previous paragraph, our SIMS results showed that there were Zn-Si inter-diffusion at the ZnO/SiO_2 interface of the as-grown samples and the inter-diffusion would be significantly enhanced by thermal annealing. Studying the near-interfacial defects of oxide/ZnO interface, Wang *et al*.[27] also showed that deep level defects were easily formed at the near-interfacial region, and it had the effect of enhancing the defect emission. In the present study, the 2.8 eV and the 3.0 eV peaks were only found in the $E_b = 10$ keV spectra, and were thus thought to be associated with defects located closer to the ZnO/SiO_2 interface. The 2.8 eV peak was observed in the as-grown sample, but vanished after the 400 °C annealing. The 3.0 eV peak was induced after the 1000 °C annealing. CL measurement was also conducted on the as-grown and the 1000 °C annealed SiO_2 substrate and no similar luminescence was observed, confirming that the two observed peaks were not originated from the substrate. Broad defect emission with similar peak (2.85 eV) has previously been reported in metalorganic chemical vapor deposition (MOCVD) grown O-rich ZnO.[28] The author ascribed this to the Zn_i to V_{Zn} transition,[28] though concrete evidence has not been obtained.

The 1.6 eV peak was observed in both the $E_b = 5$ keV and 10 keV CL spectra. Irrespective of E_b, annealing at $T_{anneal} \leq 800$ °C had an effect of enhancing the peak intensity, which then saturated at 1000 °C annealing. Ong *et al*.[29] has reported a close-by CL peak of 1.69 eV, which was attributed to defect or the second order band edge emissions.

The broad peak centered at ~2.4 eV observed in both the $E_b = 5$ keV and 10 keV spectra was commonly termed the green luminescence GL. The origin of the GL is still controversial. Structureless GL emission has been associated with V_O (Refs. 30–32) and V_{Zn}.[25,33] In the present study, the annealing behavior of the GL was independent of the electron beam energy E_b. The GL was not found in the as-grown sample. Irrespective of the electron beam energy (as shown in Fig. 5), annealing the sample at 800 °C would induce significant GL defect emission and it persisted after the 1000 °C annealing. These deep level defects associated with the GL would act as the compensating center against the *p*-type doping of the ZnO film, and would thus lead to the vanish of the *p*-type conduction property observed in the range of $T_{anneal} = 800$–1000 °C.

CONCLUSION

Using RF magnetron sputtering, As-doped ZnO films were grown on SiO_2 at a substrate temperature of 200 °C. The resultant film was initially *n*-type. It converted to *p*-type conductive after the 400 °C annealing. The formation of the *p*-type conductivity was attributed to the formation of the $As_{Zn}(V_{Zn})_2$ shallow acceptor. However, further increasing the annealing temperature decreased the hole concentration. This was explained in terms of the formation of the compensating defect associated with the GL and the dissociation of the $As_{Zn}(V_{Zn})_2$ shallow acceptor.

ACKNOWLEDGMENTS

This work was financially supported by the Research Grant Council HKSAR through the General Research Fund (GRF) (HKU7031/08P and HKU7021/10P) and The University of Hong Kong's University Development Fund (UDF) and Small Project Grant.

[1] *Zinc Oxide Bulk, Thin Films and Nanostructures Processing, Properties and Applications*, edited by C. Jagadish and S. J. Pearton (Elsevier, New York, 2006).
[2] Ü. Özgür, Ya. I. Alivov, C. Liu, A. Teke, M. A. Reshchikov, S. Doğan, V. Avrutin, S.-J. Cho and H. Morkoç, J. Appl. Phys. **98**, 041301 (2005).
[3] D. C. Look, Phys. Status Solidi B **241**, 624 (2004).
[4] V. Avrutin, D. J. Silversmith, and H. Morkoç, Proc. IEEE **98**, 1269 (2010).
[5] *Positron Beams and Their Applications*, edited by P. Coleman (World Scientific, Singapore, 2000).
[6] R. Krause-Rehberg and H. S. Leipner, *Positron Annihilation in Semiconductors-Defect Studies* (Springer, Berlin, 1999).
[7] S. Brunner, W. Puff, A. G. Balogh, P. Mascher, W. Triftshauser, G. Kogel, and P. Sperr, Mater. Sci. Forum **363-3**, 141 (2001).
[8] F. Tuomisto, V. Ranki, K. Saarinen, and D. C. Look, Phys. Rev. Lett. **91**, 205502 (2003).
[9] Z. Q. Chen, S. J. Wang, M. Maekawa, A. Kawasuso, H. Naramoto, X. L. Yuan, and T. Sekiguchi, Phys. Rev. B **75**, 245206 (2007).
[10] G. Brauer, W. Anwand, D. Grambole, J. Grenzer, W. Skorupa, J. Čižek, J. Kuriplach, I. Procházka, C. C. Ling, C. K. So, D. Schulz, and D. Klimm, Phys. Rev. B **79**, 115212 (2009).
[11] W. Anwand, G. Brauer, R. I. Grynszpan, T. E. Cowan, D. Schulz, D. Klimm, J. Čižek, J. Kuriplach, I. Procházka, C. C. Ling, A. B. Djurišić, V. Klemm, G. Schreiber, and D. Rafaja, J. Appl. Phys. **109**, 063516 (2011).
[12] A. Uedono, T. Koida, A. Tsukazaki, M. Kawasaki, Z. Q. Chen, S. Chichibu, and H. Koinuma, J. Appl. Phys. **93**, 2481 (2003).
[13] T. Koida, S. F. Chichibu, A. Uedono, A. Tsukazaki, M. Kawasaki, T. Sota, Y. Segawa, and H. Koinuma, Appl. Phys. Lett. **82**, 532 (2003).
[14] J. C. Fan, C. Y. Zhu, S. Fung, Y. C. Zhong, K. S. Wong, Z. Xie, G. Brauer, W. Anwand, W. Skourpa, C. K. To, B. Yang, C. D. Beling, and C. C. Ling, J. Appl. Phys. **106**, 073709 (2009).
[15] K. H. Tam, C. K. Cheung, Y. H. Leung, A. B. Djurišić, C. C. Ling, C. D. Beling, S. Fung, W. M. Kowk, W. K. Chan, D. L. Philips, L. Ding, and W. K. Ge, J. Phys. Chem. B **110**, 20865 (2006).
[16] Y. F. Hsu, Y. Y. Xi, K. H. Tam, A. B. Djurišić, J. M. Luo, C. C. Ling, C. K. Cheung, A. M. C. Ng, W. K. Chan, X. Deng, C. D. Beling, S. Fung, K. W. Cheah, P. W. K. Fong, and C. C. Surya, Adv. Funct. Mater. **18**, 1020 (2008).
[17] Q. L. Gu, C. C. Ling, X. D. Chen, C. K. Cheung, A. M. C. Ng, C. D. Beling, S. Fung, A. B. Djurišić, L. W. Lu, G. Brauer, and H. C. Ong, Appl. Phys. Lett. **90**, 122101 (2007).
[18] Q. L. Gu, C. K. Cheung, C. C. Ling, A. M. C. Ng, A. B. Djurišić, L. W. Lu, X. D. Chen, S. Fung, C. D. Beling, and H. C. Ong, J. Appl. Phys. **103**, 093706 (2008).
[19] G. Brauer, W. Anwand, W. Skorupa, J. Kuriplach, O. Meliknova, C. Moisson, H. Von Wenckstern, H. Schmidt, M. Lorenz, and M. Grundmann, Phys. Rev. B **74**, 045208 (2006).
[20] Z. Q. Chen, A. Kawasuso, Y. Xu, H. Naramoto, X. L. Yuan, T. Sekiguchi, R. Suzuki, and T. Ohdaira, J. Appl. Phys. **97**, 013528 (2005).
[21] M. Khalid, M. Zlese, A. Setzer, P. Esquinazi, M. Lorenz, H. Hochmuth, M. Grundmann, D. Spemann, T. Butz, G. Brauer, W. Anwand, G. Fisher, W. A. Adeagbo, W. Hergert, and A. Emst, Phys. Rev. B **80**, 035331 (2009).
[22] J. C. Fan, G. W. Ding, S. Fung, Z. Xie, Y. C. Zhong, K. S. Wong, G. Brauer, W. Anwand, D. Grambole, and C. C. Ling, Semicond. Sci. Technol. **25**, 085009 (2010).
[23] A. van Veen, H. Schut, J. de Vries, R. A. Hakvoort, and M. R. Ijpma, AIP Conf. Proc. **218**, 171 (1990).
[24] S. Limpijumnong, S. B. Zhang, S.-H. Wei, and C. H. Park, Phys. Rev. Lett. **89**, 222113 (2006).
[25] Anderson Janotti and C. G. Van de Walle, Phys. Rev. B **76**, 165202 (2007).
[26] T. E. Everhart and P. H. Hoff, J. Appl. Phys. **42**, 5837 (1971).
[27] R. S. Wang, Q. L. Gu, C. C. Ling, and H. C. Ong, Appl. Phys. Lett. **92**, 042106 (2008).

Downloaded 15 Mar 2012 to 147.8.21.150. Redistribution subject to AIP license or copyright; see http://jap.aip.org/about/rights_and_permissions

[28]C. H. Ahn, Y. Y. Kim, D. C. Kim, S. K. Mohanta, and H. K. Cho, J. Appl. Phys. **105**, 013502 (2009).
[29]H. C. Ong, A. S. K. Li, and G. T. Du, Appl. Phys. Lett. **78**, 2667 (2001).
[30]K. Vanheusden, C. H. Seager, W. L. Warren, D. R. Tallant, and J. A. Voigt, Appl. Phys. Lett. **68**, 403 (1996).
[31]S. A. Studenikin, N. Golego, and M. Cocivera, J. Appl. Phys. **84**, 2287 (1998).
[32]F. H. Leiter, H. R. Alves, A. Hofstaetter, D. M. Hoffmann, and B. K. Meyer, Phys. Status. Solidi B **226**, R4 (2001).
[33]D. C. Reynolds, D. C. Look, B. Jogai, and H. Morkoç, Solid State Commun. **101**, 643 (1997).

Downloaded 15 Mar 2012 to 147.8.21.150. Redistribution subject to AIP license or copyright; see http://jap.aip.org/about/rights_and_permissions